Available online at www.sciencedirect.com

ScienceDirect

Solar Energy xxx (2013) xxx–xxx

SOLAR ENERGY

www.elsevier.com/locate/solener

# Plasmonic effect of gold nanoparticles in organic solar cells

Marco Notarianni [a], Kristy Vernon [a], Alison Chou [a], Muhsen Aljada [b], Jinzhang Liu [a], Nunzio Motta [a,*]

[a] School of Chemistry, Physics, and Mechanical Engineering, Queensland University of Technology, Brisbane 4001, Australia
[b] Centre for Organic Photonics & Electronics, University of Queensland, Brisbane 4072, Australia

Communicated by: Associate Editor Smagul Zh. Karazhanov

**Abstract**

Light trapping, due to the embedding of metallic nanoparticles, has been shown to be beneficial for a better photoabsorption in organic solar cells. Researchers in plasmonics and in the organic photovoltaics fields are working together to improve the absorption of sunlight and the photon–electron coupling to boost the performance of the devices.

Recent advances in the field of plasmonics for organic solar cells focus on the incorporation of gold nanoparticles. This article reviews the different methods to produce and embed gold nanoparticles into organic solar cells. In particular, concentration, size and geometry of gold nanoparticles are key factors that directly influence the light absorption in the devices. It is shown that a careful choice of size, concentration and location of gold nanoparticles in the device result in an enhancement of the power conversion efficiencies when compared to standard organic solar cell devices.

Our latest results on gold nanoparticles embedded in on organic solar cell devices are included. We demonstrate that embedded gold nanoparticles, created by depositing and annealing a gold film on transparent electrode, generate a plasmonic effect which can be exploited to increase the power conversion efficiency of a bulk heterojunction solar cell up to 10%.


*Keywords:* Gold nanoparticles; Organic solar cell; Surface plasmon; Bulk heterojunction

## 1. Introduction

Organic photovoltaics developed rapidly in the last decade due to its potential to achieve a faster, lower-cost and larger volume process to manufacture devices compared to the silicon technology (Kalowekamo and Baker, 2009; Powell et al., 2009). Specifically, the potential of printing or coating solar cells, using roll to roll machinery, makes this technology very attractive for future mass production (Kippelen and Brédas, 2009; Krebs, 2009a,b).

The power conversion efficiency (PCE) (Dennler et al., 2009), the device lifetime (Jørgensen et al., 2008) and the large scale production (Brabec and Durrant, 2008) are three problems that sill need to be solved in this technology in order to compete with the technologies already present on the market.

The PCE in organic solar cells is controlled by the absorption of light and the collection of charges at the electrodes (Schilinsky et al., 2002). Increasing the light absorption is crucial in order to increase the PCE of these devices. Due to low carrier mobilities of the conducting polymer (Street et al., 2010) and short lifetime of the excitons (Halls et al., 1996; Theander et al., 2000), the optimum thickness of the active layer is often limited to ~100 nm or less (Kirchartz et al., 2012; Min Nam et al., 2010; Namkoong et al., 2013). For larger thicknesses, the recombination of free charge carriers becomes predominant with a consequent decrease of the PCE. Lowering the thickness limits the

* Corresponding author. Tel.: +61 7 3138 5104.
*E-mail address:* n.motta@qut.edu.au (N. Motta).

0038-092X/$ - see front matter © 2013 Elsevier Ltd. All rights reserved.
http://dx.doi.org/10.1016/j.solener.2013.09.026

absorption of all the photons with a consequent low photocurrent.

For these reasons, increasing the optical path length of the light in the device becomes crucial in order to increase the PCE. In fact, the increase by guiding the light multiple times in the active layer of the organic solar cells can increase the absorption probability in the device (Mokkapati and Catchpole, 2012). The light trapping can be achieved with structures that are similar or smaller in size to the wavelength of the light of interest and with specific materials that interact strongly with the light such as semiconductors or metals.

In particular, collective oscillation of electrons in metallic nanoparticles are generated by the light at a specific frequency leading to a strong absorption or scattering of the light as function of particle size (Catchpole et al., 2011). Metallic nanoparticles have already been used to enhance the photocurrent by 33% of thin film silicon solar cells (Pillai et al., 2007).

Recently, the usage of the metallic nanoparticles in organic photovoltaics has been exploited because they can be easily incorporated without compromising the architecture of the device.

This review article presents a summary of organic photovoltaics, a description of the physical mechanisms of light trapping in organic solar cells through metallic nanoparticles and recent results on the incorporation of gold nanoparticles in organic photovoltaics devices.

## 2. Organic photovoltaics

A typical organic solar cell is composed of different layers that can be organic and/or inorganic. A solar cell is defined as organic if the active absorbing layer is composed by only organic material. The most common structure of an organic solar cell consists of two electrodes (in which one of the two has to be transparent) with an active layer between them, where the generation of free charge carriers will occur. Sometimes, a buffer layer is included between each electrode and the active layer, to ensure that a charge selective transport occurs preventing charge recombination effects that reduce the performance of the device.

The generation of a photocurrent from an incident light in organic solar cells can be summarized in the following way: photon absorption in the conducting polymer; creation of an exciton (bound state of an electron and a hole which are attracted to each other by the electrostatic Coulomb force); exciton separation at the interface of the heterojunction (interface between the donor and the acceptor material). Due to the built-in electric field at the interface of the heterojunction, the electron is transferred to the acceptor material and the hole to the donor material causing the creation of a photocurrent (Krebs, 2010; Nunzi, 2002).

The excitons generated by the light typically have very short lifetimes with a recombination distance between 4 nm and 20 nm (Halls et al., 1996; Theander et al., 2000). Because of this problem, the bulk heterojunction (BHJ) solar cell (mixture of the donor and acceptor material) is the best solution in terms of performance because it provides a larger volume of interaction between the acceptor and the donor, more efficient charge separation and separate paths for the transport of free carriers (Erb et al., 2005; Li et al., 2005; Mihailetchi et al., 2005). The first kind of BHJ solar cell was originally proposed by Sariciftci et al. (1992). It was composed of on an active layer made out of a conducting polymer that was the electron donor material mixed with fullerenes derivatives that was the electron acceptor material (Umnov and Korovyanko, 2005). The active layer morphology is an important parameter to be considered for the performance of the device (Pivrikas et al., 2011; Su et al., 2012; Watkins et al., 2005).

At present, the most studied BHJ solar cells are the ones based on fullerene derivative [6,6]-phenyl-C61-butyric acid methyl ester (PCBM) as acceptor material and conducting polymer poly(3-hexylthiophene-2,5-diyl) (P3HT) as donor material (Lee et al., 2011; Seemann et al., 2011; Tao et al., 2013). P3HT and PCBM have been commonly used as reference materials for organic solar cells because they are readily commercially available and guarantee stable devices. In the regular structure (Fig. 1a), Indium Tin Oxide (ITO) is mostly used as the transparent conducting anode, poly(3,4-ethylenedioxythiophene):poly(styrene sulfonate) (PEDOT:PSS) is the electron blocking layer, lithium fluoride (LiF) is the hole blocking layer and aluminum (Al), is used as the cathode because of its low work function (Bindl et al., 2011; Nelson, 2011). In this device, the holes are collected at the ITO and the electrons are collected at the Al electrode. This structure can be reversed (Fig. 1b) by inserting a hole blocking layer between the ITO and the active layer in order to collect electrons at the ITO electrode and inserting an electron blocking layer on the metal electrode in order to collect holes. The metal electrode in this case is made of a high work function metal that is usually gold or silver. A typical inverted structure is composed of ITO as the cathode, zinc oxide (ZnO) as the hole blocking layer, PCBM:P3HT as the active layer, the PEDOT:PSS as the electron blocking layer and gold (Au) as the anode (Hau et al., 2010).

Currently, many stable devices based on the P3HT:PCBM mixture have a PCE of about 4% (Dang et al., 2011). Some research groups are replacing the PCBM with other fullerene derivatives, such as phenyl-C71-butyric acid methyl ester ($PC_{71}BM$), obtaining PCEs higher than 7% (Liang et al., 2010). After the discovery of the high carrier mobility, intrinsic one-dimensionality, and tuneable optical and electronic properties of carbon nanotubes (CNTs) (Zhu et al., 2009), many groups are trying to use this material in organic solar cells (Sgobba and Guldi, 2008). Some groups are trying to replace either partially (Lu et al., 2013) or completely (Ren et al., 2011) the PCBM compounds with carbon nanotubes (CNTs). In particular, they observed that when the P3HT is mixed with the CNTs, the polymer chains tend to wrap the CNTs

Please cite this article in press as: Notarianni, M., et al. Plasmonic effect of gold nanoparticles in organic solar cells. Sol. Energy (2013), http://dx.doi.org/10.1016/j.solener.2013.09.026

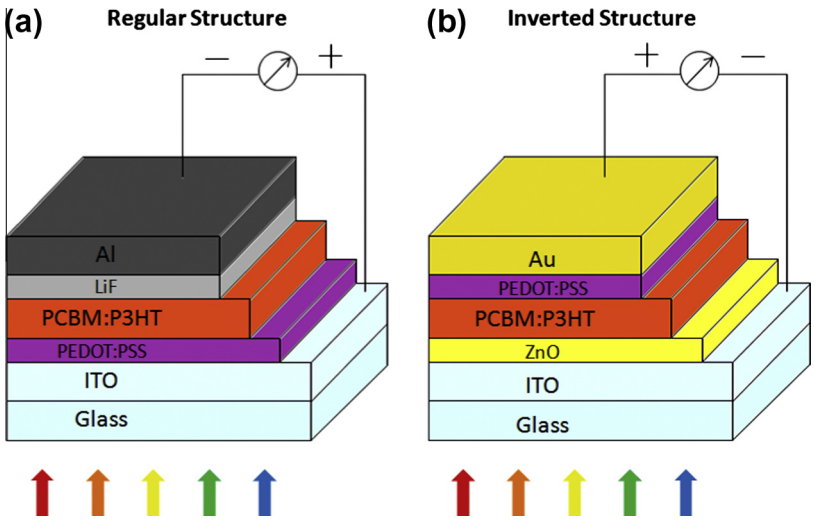


Fig. 1. (a) Schematic of a regular organic solar cell structure. (b) Schematic of an inverted organic solar cell structure.

(Giulianini et al., 2011a,b, 2009) with an electron transfer between the CNTs and the P3HT (Bernardi et al., 2010). Others are trying to replace the PEDOT:PSS buffer layer, because of its hygroscopicity and acidity that causes degradation of the active layer and the ITO electrode (Sun et al., 2010; Wong et al., 2012), with carbon nanotubes (CNTs) (Capasso et al., 2012) or a blend of CNTs:P3HT (Dabera et al., 2012) because of its hygroscopicity and acidity that causes degradation of the active layer and the ITO electrode resulting in a decreased lifetime of the solar cell device (Sun et al., 2010). Others are replacing the ITO with CNTs film electrodes because of their optical transparency and high conductivity properties (Mirri et al., 2012; Sears et al., 2013).

Other research groups are working on the synthesis of new conducting polymers that are able to absorb a larger portion of the solar spectrum. In fact, P3HT, which is largely used in organic solar cells, has an absorption spectrum poorly matching the solar emission spectrum. For this reason the P3HT, is able to collect only up to 22.4% of the available solar photons (Bundgaard and Krebs, 2007; Smestad et al., 2008). In particular, conducting polymers with a low band gap are recently being used in order to increase the PCE (Liang et al., 2009; Peet et al., 2007; Zhu et al., 2007).

Other groups are working on combining low band gap polymers with high band gap polymers in a specific device called a tandem organic solar cell achieving efficiencies higher than 10% (Dou et al., 2012; You et al., 2013). This device is composed of several layers including two active layers, one with a low band gap and one with a high band gap polymer able to collect photons in two matching spectral ranges, increasing the overall light absorption (Ameri et al., 2009; Hadipour et al., 2008) (Fig. 2). The latest reported PCE record of 12% was achieved this year by Heliatek with a tandem organic solar cell (Heliatek Firm, 2013).

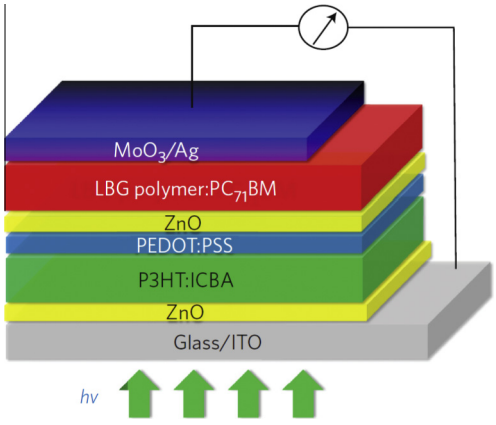


Fig. 2. Device structure of an inverted tandem solar cell (LBG, low bandgap polymer). Reproduced with permission from (Wu et al., 2011). Copyright 2012 Nature Photonics.

Despite the use of new compounds in the active layer or in the buffer layers and to the implementation of new architectures, the PCE is still limited by the low photon absorption in the active layer. At present, while tandem organic solar cells structures represent a sure way to achieve a maximum spectral range for the photoabsorption in the device, they do not provide a valid mechanism to obtain the most by the incoming photons in terms of light-electrons conversion. The introduction of plasmonic structures such as metallic nanoparticles can also be a valid strategy to improve the PCE in organic photovoltaics devices by improving the coupling between the light and the matter.

## 3. Plasmonic light trapping in organic solar cells

Light trapping in organic solar cells has become an interesting solution to increase the PCE in organic solar cell devices similarly to what was realized with thin film silicon solar cell technology where the thickness of the silicon

Please cite this article in press as: Notarianni, M., et al. Plasmonic effect of gold nanoparticles in organic solar cells. Sol. Energy (2013), http://dx.doi.org/10.1016/j.solener.2013.09.026

is only a few micrometers (Derkacs et al., 2006; Pillai et al., 2007) or similarly to what was done to enhance the performance of dye-sensitized solar cells (Lin et al., 2012; Muduli et al., 2012).

Several techniques have been proposed for light trapping in organic photovoltaics such as the inclusion of periodic nanostructures (Kang et al., 2010; Mariani et al., 2010; Zeng et al., 2013), diffraction gratings (Lindquist et al., 2008; Niggemann et al., 2004), metallic nanoparticles (Kim et al., 2008; Lu et al., 2012; Morfa et al., 2008; Wu et al., 2011) and a combination of gratings and metallic nanoparticles (Li et al., 2012). The use of metallic nanoparticles does not compromise the architecture of the devices because they can be easily added to one of the organic solar cell layers.

Specifically, the inclusion of metallic nanoparticles can enhance the absorption of the light by two mechanisms: an increasing of the forward scattering cross section and a near-field enhancement (Atwater and Polman, 2010) (Fig. 3).

In particular, when the metallic particles are very similar or smaller in size than the wavelength of the light of interest, a strong interaction occurs between the free conduction electrons in the metal and the electromagnetic radiation. Plasmons are the oscillations of these free conductions electrons with the generation of a dipole into the particles due to the interaction with the light (Fig. 4). The resonance condition occurs when the frequency of the light matches the frequency of the electrons oscillating and is defined as localized surface plasmon resonance (LSPR) in the case of nanometer sized structures.

The plasmon energy in a free electron model is defined as (Maier, 2007):

$$E_p = \hbar\sqrt{\frac{ne^2}{m\varepsilon_0}} = \hbar\omega_p \tag{1}$$

where $n$ is the density of free electrons, $e$ is the elementary charge, $m$ is the electron mass, $\varepsilon_0$ the permittivity of free space, $\hbar$ is the Planck constant and $\omega_p$ the bulk plasmon frequency.

For metals with low interband absorption, the dielectric function can be described by the Drude model, which explains the response of damped, free electrons to an

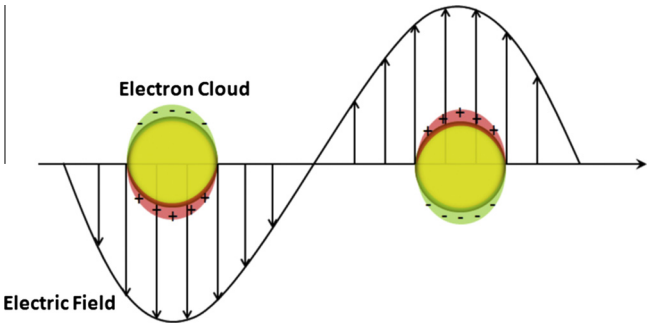


Fig. 4. Schematic of surface plasmon resonance where the free conduction electrons in the metal nanoparticle are driven into oscillation due to strong coupling with incident light.

applied electromagnetic field with a frequency of $\omega$ (Maier, 2007):

$$\varepsilon_r(\omega) = 1 - \frac{\omega_p}{\omega^2 + i\gamma\omega} \tag{2}$$

where $\tau = \frac{1}{\gamma}$ is the relaxation time and $\omega$ is the angular frequency of an applied electromagnetic field.

A metallic nanoparticle embedded in a homogeneous medium scatters the light in both forward and reverse directions (Bohren and Huffman, 2008; Kreibig and Vollmer, 1995). Instead, the light will scatter more into the dielectric with larger permittivity (Mertz, 2000) if the nanoparticle is placed close to the interface of two dielectrics. In this way, the optical path length can be increased by the angular spread of the light into the dielectric (Viktor Andersson et al., 2011). The metal contact reflects the light back towards the surface, where the metallic nanoparticles are present, causing the light to scatter again resulting in multiple passes of the light through the organic solar cell (Fig. 3a).

For metallic nanoparticles with diameters below the wavelength of the light, a point dipole model describes both the absorption and the scattering of the electromagnetic field. The scattering and absorption cross-sections are given by Huffman and Bohren (1983):

$$C_{scat} = \frac{1}{6\pi}\left(\frac{2\pi}{\lambda}\right)^4 |\alpha|^2; \quad C_{abs} = \frac{2\pi}{\lambda}\mathrm{Im}[\alpha] \tag{3}$$

with

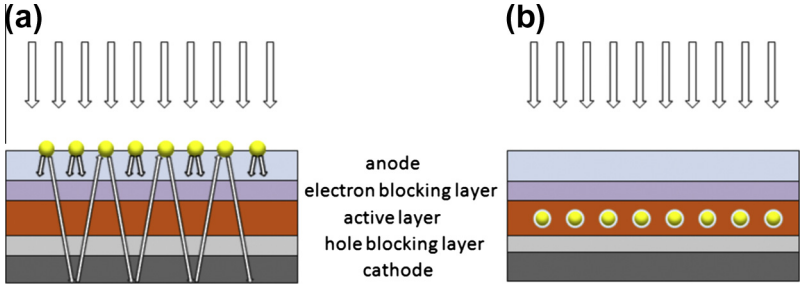


Fig. 3. (a) Light trapping by scattering from metallic nanoparticles at the surface of a standard organic solar cell. The optical path length is increased because light is trapped into the device through multiple angle scattering. (b) Excitation of localized surface plasmons in metallic nanoparticles embedded in the organic solar cell.

Please cite this article in press as: Notarianni, M., et al. Plasmonic effect of gold nanoparticles in organic solar cells. Sol. Energy (2013), http://dx.doi.org/10.1016/j.solener.2013.09.026

$$\alpha = 3V\frac{\omega_p^2}{\omega_p^2 - 3\omega^2 - i\gamma\omega} = 3V\left[\frac{\varepsilon_p/\varepsilon_m - 1}{\varepsilon_p/\varepsilon_m + 2}\right] \quad (4)$$

where $\alpha$ is the polarizability of the particle, $V$ is the particle volume, $\varepsilon_p$ is the dielectric function of the particle and $\varepsilon_m$ is the dielectric function of the embedding medium. If $\varepsilon_p = -2\varepsilon_m$, the particle polarizability will become very large (Huffman and Bohren, 1983). This occurs when the frequency is close to the surface plasmon resonance $\omega_{sp}$, allowing the light to interact over an area larger than the geometric cross section of the particle (Bohren and Craig, 1983).

In the case of a spherical structure the surface plasmon occurs at $\omega_{sp} = 1\sqrt{3\omega_p}$.

The scattering efficiency is given by the formula (Bohren and Huffman, 2008):

$$Q_{scat} = C_{scat}/(C_{scat} + C_{abs}) \quad (5)$$

For example, at resonance, small silver nanoparticles in air have a scattering cross section that is around ten times the cross sectional area of the particle. This means that just a substrate covered with only 10% of the particles could fully absorb and scatter the incident light (Catchpole and Polman, 2008b). For light trapping caused by a scattering effect, it is important to increase the scattering cross section rather than the absorption. This effect can be achieved with large particles of 100 nm size or more. Other parameters such as the shape, material of the particles and surrounding medium can also contribute to increase the scattering effect in the organic solar cell device (Atwater and Polman, 2010; Derkacs et al., 2008; Jain et al., 2006; Kelly et al., 2002; van Dijk et al., 2006). For example, taking a range of gold nanoparticles sitting on an ITO substrate coated with PEDOT:PSS and using Lumerical FDTD it is possible to determine the amount of light scattered into the PEDOT:PSS for various shapes and sizes of the nanoparticles. As can be seen, the amount of light scattered into the PEDOT: PSS is directly affected by the size and the shape of the particle (Fig. 5).

Another way to benefit from the resonant plasmon excitation in an organic solar cell is to take advantage of the strong local field enhancement around the metallic nanoparticles in order to increase the light absorption in the surrounding area (Fig. 3b). When the Au NPs are very similar or smaller in size (5–50 nm) to the wavelength of light, they can act as antennas for the incident light storing the energy in a localized surface plasmon modes with up to 100 times enhancement of the electric field (Duche et al., 2009; Rand et al., 2004; Shen et al., 2009). Simulations show the generation of a strong near field distribution around the Au NPs when immersed in the active layer with a consequent enhancement of the light absorption (Wang et al., 2012; Xie et al., 2011) (Fig. 6). These antennas are particularly useful in materials where the carrier diffusion lengths are small like the conducting polymers where the exciton lifetime is very short. In fact, the absorption rate has to be larger than the reciprocal of the plasmon decay time (lifetime

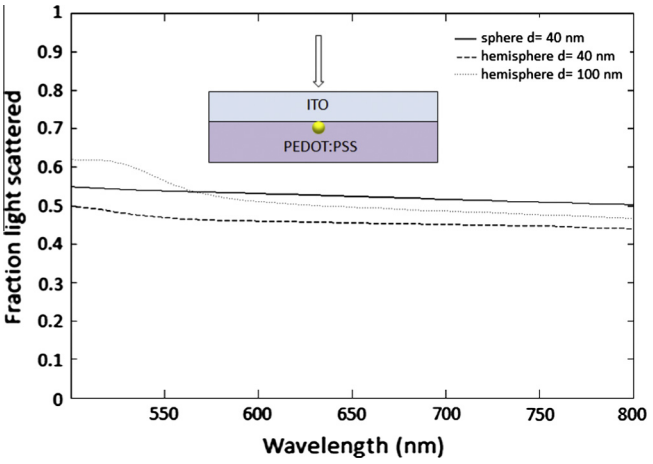


Fig. 5. Schematic of the system and calculation of the fraction of incident light scattered into the PEDOT:PSS for a gold sphere of 40 nm diameter, a gold hemisphere of 40 nm diameter and a gold hemisphere of 100 nm diameter deposited on the ITO substrate.

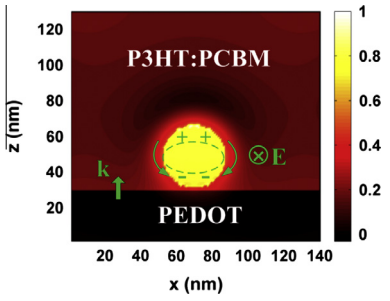


Fig. 6. Schematic pattern for the plasmon resonance and charge distribution of a Au NPs, as well as the near field distributions for the vertically incident light with the TE polarization in P3HT:PCBM. Reproduced with permission from (Xie et al., 2011). Copyright 2008 AIP.

~10–50 fs) otherwise the energy absorbed is dissipated into ohmic damping in the metal (Atwater and Polman, 2010). These plasmonic structures embedded in the actie layer can modify the coupling between plasmon and exciton resulting in the generation of hot excitons (Wu et al., 2011). The generation of these hot excitons can increase the generation of free charges (Grancini et al., 2013; Kambhampati, 2011; Ohkita et al., 2008) reducing thereby the recombination of excitons through radiative and non-radiative processes with a resulting increase of the efficiency of the device (Lee et al., 2009) (Fig. 7).

Metallic nanoparticles are usually made of aluminum, silver, gold or copper because these metals strongly interact with the sunlight. Specifically, aluminum and silver lead to surface plasmons resonance in the ultraviolet spectrum while gold and copper lead to surface plasmons resonance in the visible spectrum (Catchpole and Polman, 2008a). Generally, silver is preferred for its low cost and low absorption but gold is recently largely used because it is widely believed that it does not suffer from oxidation effects and so guarantees long life to the device. Unfortunately, at the nanoscale gold clusters have the ability to act as an exothermic center absorbing multiple molecules of oxygen

Please cite this article in press as: Notarianni, M., et al. Plasmonic effect of gold nanoparticles in organic solar cells. Sol. Energy (2013), http://dx.doi.org/10.1016/j.solener.2013.09.026

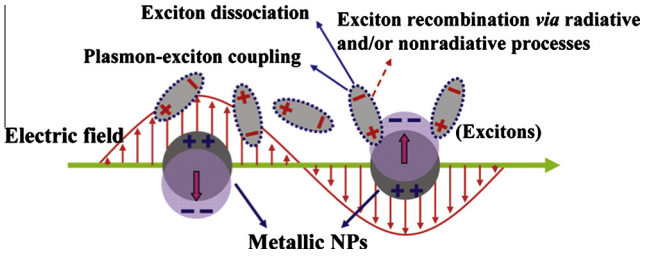


Fig. 7. Cartoon depiction of the interaction between the localized surface plasmon resonance and the excitons. The interaction enhances the rate of exciton dissociation thereby reducing the exciton recombination. Reproduced with permission from (Wu et al., 2011). Copyright 2011 ACS Nano.

(Frondelius et al., 2010; Sanchez et al., 1999; Sutter et al., 2013). Therefore, it is not possible to rule out oxidation effects in Au NPs.

## 4. Synthesis of gold nanoparticles for organic solar cells

Gold nanoparticles (Au NPs) can be produced by liquid chemical method (Louis and Pluchery, 2012), by ablation in liquids with pico and femtosecond laser pulses (Yang, 2012) and by deposition of gold on a substrate followed by thermal annealing (Pillai et al., 2007).

In the liquid chemical method, the Au NPs are created by the reduction of a precursor. Gold halides are the precursors commonly used in this case and are prepared by dissolution of bulk gold in aqua regia or metal cyanide with the formation of the chloroauric acid ($HAuCl_4$) or gold chloride ($AuCl_3$). Under controlled conditions, reducing agents are added to the precursor solution. A proper choice of the reducing agent is important to synthesize regular nanoparticles with a narrow shape and size distribution (Louis and Pluchery, 2012). Other important parameters that control the size distribution of the particles are ageing time, concentration, nature of different constituents and reduction technique (Louis and Pluchery, 2012). The citrate reduction method is one of the most common to synthesize spherical Au NPs (Frens, 1973; Turkevich et al., 1951). Fig. 8 shows an example of Au NPs produced by the citrate reduction method. Specifically, 20 mL of a 4% solution of sodium citrate was added to 100 mL of 4 mM $HAuCl_4$ at 90 °C (Chou et al., 2012). The mixture was kept at 90 °C with stirring for 20 min and cooled to room temperature before use. The size of the Au NPs can be controlled by varying the citrate/gold precursor concentration ratio and the result can be even observed by the color change of the solutions (Fig. 8).

The size of the Au NPs can be estimated from the UV–Vis spectra. In particular, the diameter $d$ in nm of the particle is given by the following formula (Haiss et al., 2007):

$$d = \frac{\ln\left(\frac{\lambda_{spr}-\lambda_0}{L_1}\right)}{L_2} \quad (6)$$

where $\lambda_0 = 512$ nm; $L_1 = 6.53$ nm; $L_2 = 0.0216$ nm$^{-1}$ are parameters determined from the theoretical model, while

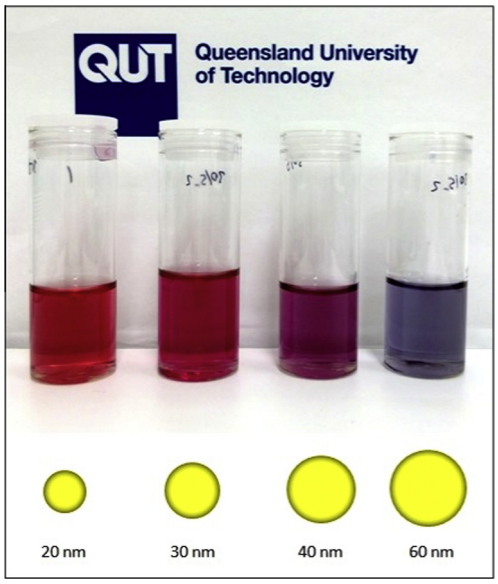


Fig. 8. Solutions of Au NPs of various sizes (20–60 nm). The size difference causes the difference in colors.

$\lambda_{spr}$ is the wavelength in nm that corresponds to the maximum absorbance peak obtained from the UV–Vis spectra of the samples (Haiss et al., 2007). In this way (Fig. 9), it is possible to deduce the size of the Au NPs produced. The optical properties of spherical gold nanoparticles are a function of their size. As the diameter of nanoparticle increases, the maximum extinction wavelength shifts to longer wavelength and broadens as the ratio of nanoparticle scattering to total extinction increases, SEM images in Fig. 10 confirm the size of the Au NPs determined by UV–Vis spectra.

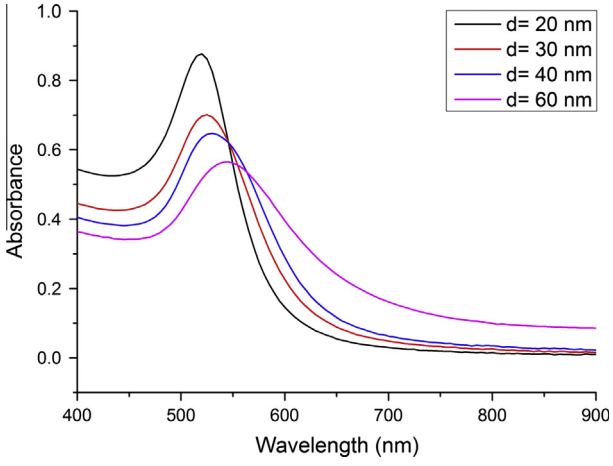


Fig. 9. UV–Vis spectra of Au NPs of different sizes produced by Turckevich method. From the position of the main peak it is possible to determine the average particle diameter. $\lambda_{spr} = 522$ nm (black curve), $d = 20$ nm; $\lambda_{spr} = 525$ nm (red curve), $d = 30$ nm; $\lambda_{spr} = 528$ nm (blue curve), $d = 40$ nm; $\lambda_{spr} = 535$ nm (purple curve), $d = 60$ nm. (For interpretation of the references to color in this figure legend, the reader is referred to the web version of this article.)

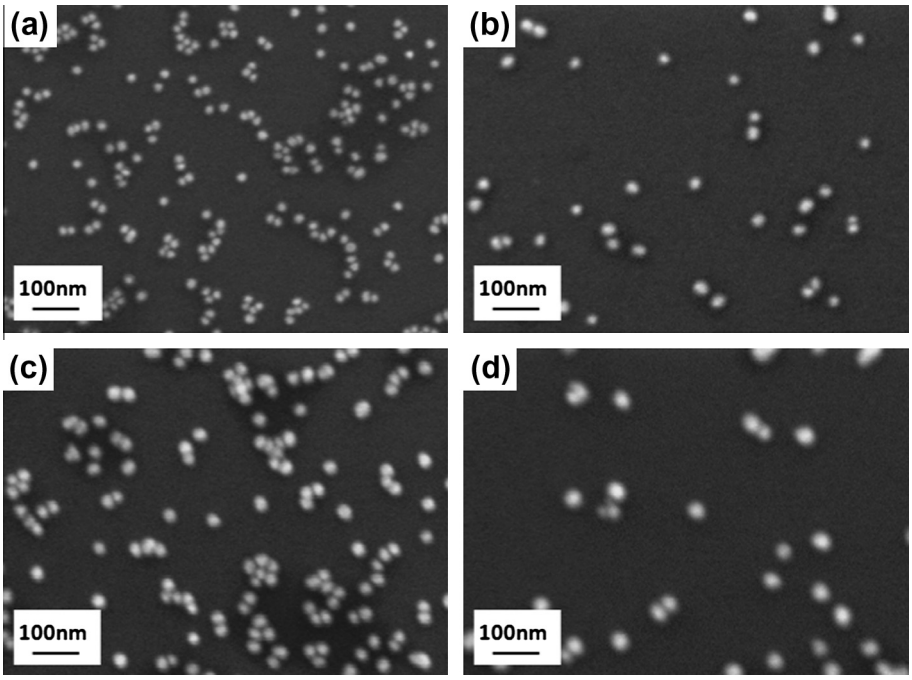


Fig. 10. SEM images Au NPs produced by chemical method. Each image corresponds to a different average particle size depending on the amount of reducing agent used. (a) Au NPs of 20 nm; (b) Au NPs of 30 nm; (c) Au NPs of 40 nm; (d) Au NPs of 60 nm.

Au NPs produced by citrate reduction usually disperse easily in a polar solvent such as water due to the negative surface charge from the citrate ions on the surface of gold nanoparticles.

Laser ablation method is recently attracting a lot of interest because of the larger availability of lasers in many laboratories and because of the possibility to produce Au NPs in liquid without the drawback of reducing agents residuals (Yang, 2012). For this reason, it is considered a reliable alternative to the liquid chemical method in order to avoid surfactants and passivation layers that could promote an undesirable exciton quenching, decreasing the plasmonic effect. The method consists in focusing a laser beam onto a solid target covered by a layer of liquid, which must be transparent at the laser wavelength. A number of parameters such as peak power, average power, wavelength emission and pulse repetition rate are crucial in order to determine the size and shape of the Au NPs. Also the thickness of the liquid layer above the target is an important experimental parameter that can influence the properties of the Au NPs (Yang, 2012).

Another method to include Au NPs in organic solar cells without the presence of passivation layers and surfactants is to deposit a thin film (1–30 nm) of gold on the ITO substrate followed by annealing in argon atmosphere at temperatures in the range of 250–400 °C. The argon flux is necessary in order to avoid an increase in the sheet resistance of the ITO (Hamasha et al., 2012; Kim et al., 2005) due to oxygen reaction. During the annealing process, the particles merge together to form islands due to the surface tension. These islands have size and shape, which depend on the amount of gold deposited on the surface and on the annealing temperature (Fig. 10). The size and shape of the particles are also very sensitive to the surface conditions of the substrate. A similar work has been carried out by Pillai et al. (2007) and Beck et al. (2009) by depositing silver nanoparticles to improve the efficiency of silicon solar cells.

## 5. Gold nanoparticles in organic solar cells

Different approaches are used to incorporate Au NPs into organic solar cells. They can be included in one of the buffer layers (Chen et al., 2009; Kao et al., 2012; Lu et al., 2012; Wang et al., 2013; Woo et al., 2012; Wu et al., 2011; Xu et al., 2013; Yang et al., 2011), in the active layer blend (Kim and Carroll, 2005; Spyropoulos et al., 2012; Wang et al., 2012), in any of the polymer layers (Xie et al., 2011) or dispersed on the ITO electrode (Shahin et al., 2012).

When the Au NPs are embedded in the buffer layer, especially in the PEDOT:PSS, the dispersion process is easy and straight forward. In fact, because the PEDOT:PSS is dispersed in an aqueous solution, Au NPs produced by liquid chemical method can be added to the PEDOT:PSS without any additional functionalization, maintaining a good dispersion and uniformity in the solution. Woo et al. (2012), for example, showed that the Au NPs can be prepared directly in the PEDOT:PSS solution without using a stabilizer or an additional mixing step, reducing chloroauric acid ($HAuCl_4$) with sodium borohydride ($NaBH_4$) directly in the PEDOT:PSS aqueous solution. They obtained a PCE of 3.19% in a device ITO/PEDOT:PSS/P3HT:PCBM/LiF/Al incorporating Au

Please cite this article in press as: Notarianni, M., et al. Plasmonic effect of gold nanoparticles in organic solar cells. Sol. Energy (2013), http://dx.doi.org/10.1016/j.solener.2013.09.026

NPs compared to 2.95% for a device with pristine PEDOT:PSS.

Wu et al. (2011) were also able to increase the PCE from 3.57% to 4.24% with Au NPs of 50 nm in size produced by liquid chemical method were mixed to the PEDOT:PSS layer in a device ITO/PEDOT:PSS/P3HT:PCBM/Ca/Al. Lu et al. (2012) also mixed Au NPs of 40–50 nm size, in the PEDOT:PSS. In their work the PCE passed from 7.25% for the standard device ITO/PEDOT:PSS/PTB7:$PC_{71}BM$/Ca/Al to 8.16% for the plasmonic device.

Chen et al. (2009) fabricated a standard structure device ITO/PEDOT:PSS/PCBM:P3HT/Ca/Al with a concentration of 20% in volume of Au NPs in the PEDOT:PSS layer achieving PCE of 4.19%, higher than 3.48% obtained in the standard device with pristine PEDOT:PSS. For concentrations of Au NPs higher than 20% in volume, they observed a dramatic drop in the PCE. Kao et al. (2012) fabricated an inverted structure device ITO/$Cs_2CO_3$/P3HT:PCBM/$MoO_3$/Ag that achieved a record PCE of 3.54% with the inclusion of 30% in volume of 45 nm Au NPs size in the $Cs_2CO_3$ buffer layer, higher than the 3.12% PCE in the device with pristine $Cs_2CO_3$. Xu et al. (2013) increased the performance of an inverted device ITO/$TiO_2$/PTB7:$PC_{71}BM$/$MoO_3$/Al from a PCE of 6.23–7.02%, including a concentration of 30% in volume of Au NPs of 45 nm size in the $TiO_2$ layer. For lower or higher concentrations of the Au NPs, they observed a drop in the PCE. These examples show that the concentration of Au NPs is another key parameter for the final performance of the device.

Recently, other groups are trying to incorporate the Au NPs in the buffer layers of tandem organic solar cells in order to further increase the performance of the devices. Yang et al. (2011) improved the performance of a tandem device ITO/$TiO_2$:Cs/P3HT:ICBA/PEDOT/$TiO_2$:Cs/PSBTBT:$PC_{71}BM$/$MoO_3$/Al by incorporating Au NPs of 70–80 nm into the PEDOT layer. They increased the PCE from 5.22% to 6.24% with the Au NPs. Because the PEDOT layer is exactly in the middle of the cell, between the two active layers, the plasmonic effect of the Au NPs is supposed to enhance the performance of the top and bottom subcells.

The main problem in introducing Au NPs in the active layer is the fact that the organic solvent used to mix the conducting polymer and the fullerene derivatives do not disperse efficiently the Au NPs. In fact, in these cases, the Au NPs have to be functionalized with a ligand shell of other compounds such as dodecylamine (DDA), or O-[2-(3-mercaptopropionylamino)ethyl]-O'-methylpolyethylene glycol (monofunctional PEG) (Kim and Carroll, 2005; Topp et al., 2010; Wang et al., 2012). Despite the fact that another polymer is being introduced into the active layer, it has been demonstrated, particularly with the PEG, that this addition does not decrease the PCE of the device (Wang et al., 2012). In particular, Wang et al. (2012) observed an increase in the PCE from 1.64% to 2.17% with 0.5 wt% of Au NPs of 18 nm Au NPs included in the active layer of a device with a ITO/PEDOT:PSS/PFSDCN:PCBM/LiF/Al structure. When they increased the concentration of Au NPs up to 6 wt%, the photovoltaic effect was no longer observed, probably because of a short circuit between the two electrodes. The concentration of Au NPs in the active layer is still a critical parameter that can dramatically affect the efficiency of the device. In particular, when the concentration is too high, Au NPs can generate hot spots due to their dipole–dipole electromagnetic interactions, with the generation of hybridized plasmons below the surface plasmon frequency (Etchegoin et al., 2004; Pelton et al., 2008). Therefore, the excitons of the polymer and the plasmons do not interact efficiently resulting in a lower PCE (Lee et al., 2009). Kim and Carroll (2005) improved the PCE of a device ITO/PEDOT:PSS/P3OT:PCBM /Lif/Al from 1.1% to 1.7% by including Au NPs stabilized with long alkyl chain (dodecyl amine) of 6 nm in size in the active layer. Topp et al. (2010) instead found that the inclusion of 23 wt% of Au NPs functionalized with DDA in the active layer were not beneficial for the performance of the organic solar cell device. The efficiency dropped dramatically from a PCE of 2.5% in the standard device ITO/PEDOT:PSS/P3HT:PCBM/Al to 1.1% in the case of a plasmonic device with 23 wt% of Au NPs functionalized with DDA in the active layer. The reason of this drop is probably not due to the functionalization but rather to a quenching of the excited states of the polymer or to local short circuits due to aggregated Au NPs. In fact, a decrease of the PCE has to be expected if the concentration of Au NPs is too high in the active layer. (Wang et al., 2012).

Therefore, the separation of Au NPs is a crucial problem for plasmonic devices. Wang et al. (2013) showed that in order to maximize the performance of their devices they had to separate the Au NPs from the active layer with an overlayer in order to avoid quenching caused by non-radiative energy transfer to the Au NPs (Anger et al., 2006; Cheng et al., 2011). In particular, they achieved a PCE of 2.35% with an inverted structure including Au NPs and a ZnO overlayer, ITO/ZnO/AuNPs/ZnO overlayer/P3HT:PCBM/PEDOT:PSS/Ag, which is slightly better than 2.25% obtained in the same device without Au NPs and ZnO overlayer. By including only the Au NPs, the PCE was only 1.26%, much lower than in the non-plasmonic device, demonstrating that the ZnO overlayer was necessary in order to avoid this exciton quenching.

Li et al. (2012) demonstrated that the size of the Au NPs is another key parameter to be considered for the performance of the device. In fact, they tested an organic solar cell structure of ITO/$TiO_2$/PBDTTT-C-T:$PC_{71}BM$/Ag with a 2 wt% concentration of 20 nm and 50 nm Au NPs respectively in the active layer blend. A PCE of 8.11% was achieved in the device with the 50 nm Au NPs, while the 20 nm NPs device achieved only 7.83%. In both cases, the PCE was improved from the standard device that had a PCE of 7.59%.

Please cite this article in press as: Notarianni, M., et al. Plasmonic effect of gold nanoparticles in organic solar cells. Sol. Energy (2013), http://dx.doi.org/10.1016/j.solener.2013.09.026

Xie et al. (2011) proposed to incorporate the Au NPs both into the buffer and into the active layers. In fact, by using a structure ITO/PEDOT:PSS/P3HT:PCBM/LiF/Al with the Au NPs included in the PEDOT:PSS and in the P3HT:PCBM layers, they achieved a PCE of 3.85%, higher than the 3.16% from the standard device.

An easy method to embed Au NPs in organic solar cells device was proposed by Shahin et al. (2012). They just dipped the ITO electrode in a Au NPs solution. A device made of ITO/PEDOT:PSS/PCBM:P3HT/LiF/Al with the 50 nm Au NPs spread on the ITO achieved a PCE of 1.53% higher, compared 1.18% to the reference device. They also considered the effect of the Au NPs coverage establishing that if the coverage is exceeding 20%, the increased reflection effect produces a very low PCE in the device.

In order to avoid the presence of other substances in the Au NPs solution, (Spyropoulos et al., 2012) performed the synthesis of Au NPs by laser ablation method (Yang, 2012). In their work, a device with a structure ITO/PEDOT:PSS/P3HT:PCBM/Al increased its PCE from 2.64% device to 3.71% with a 5% concentration of 10 nm Au NPs dispersed in the active layer blend solution.

Table 1 lists a summary comparison of the PCE of different organic solar cells with and without Au NPs.

## 6. Plasmonic organic solar cells with gold nanoparticles formed by thermal annealing

We fabricated several plasmonic organic solar cell devices with Au NPs grown on ITO electrodes by sputtering gold followed by thermal annealing (Fig. 11) and we compared the results with a standard device without Au NPs. The structure for the plasmonic devices was ITO/PEDOT:PSS/$PC_{71}$BM:P3HT/Al with Au NPs grown on the ITO (Fig. 12).

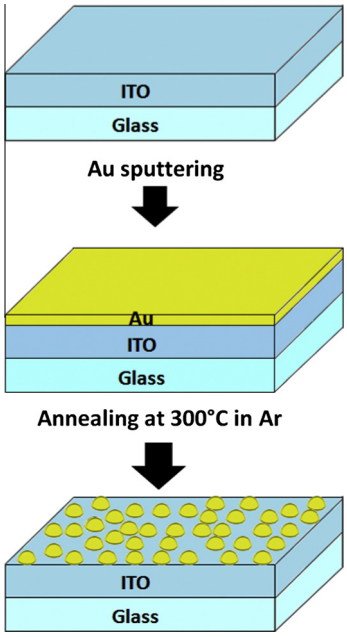


Fig. 11. Cartoon depicting the phases of gold deposition on ITO to obtain Au NPs.

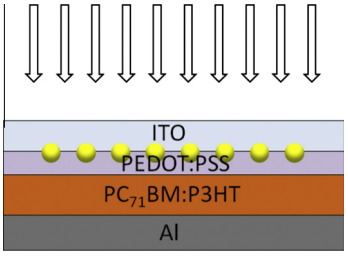


Fig. 12. Schematic of the organic solar cell device tested in this work.

In order to understand the effect of the size and shape of the Au NPs on the PCE of the devices, we used NPs

Table 1
Power conversion efficiency of organic solar cells without and with gold nanoparticles embedded in the different parts of the device.

| Device | Au NPs position | PCE (%) | | References |
|---|---|---|---|---|
| | | w/o AuNPs | With Au NPs | |
| ITO/PEDOT:PSS/P3HT:PCBM/LiF/Al | PEDOT:PSS | 2.95 | 3.19 | Woo et al. (2012) |
| ITO/PEDOT:PSS/P3HT:PCBM/Ca/Al | PEDOT:PSS | 3.57 | 4.24 | Wu et al. (2011) |
| ITO/PEDOT:PSS/P3HT:PCBM/Ca/Al | PEDOT:PSS | 3.48 | 4.19 | Chen et al. (2009) |
| ITO/$Cs_2CO_3$/P3HT:PCBM/$MoO_3$/Ag | $Cs_2CO_3$ | 3.12 | 3.54 | Kao et al. (2012) |
| ITO/$TiO_2$/PTB7:$PC_{71}$BM/$MoO_3$/Ag | $TiO_2$ | 6.23 | 7.02 | Xu et al. (2013) |
| ITO/ZnO/P3HT:PCBM/PEDOT:PSS/Ag | ZnO | 2.25 | 2.35 | Wang et al. (2013) |
| ITO/ $TiO_2$:Cs/ P3HT:ICBA /PEDOT/$TiO_2$:Cs/PSBTBT: $PC_{71}$BM /$MoO_3$/Al | PEDOT | 5.22 | 6.24 | Yang et al. (2011) |
| ITO/PEDOT:PSS/PTB7: $PC_{71}$BM /Ca/Al | PEDOT:PSS | 7.25 | 8.16 | Lu et al. (2012) |
| ITO/PEDOT:PSS/PFSDCN:PCBM/LiF/Al | PFSDCN:PCBM | 1.64 | 2.17 | Wang et al. (2012) |
| ITO/PEDOT:PSS/P3HT:PCBM /Al | P3HT:PCBM | 2.64 | 3.71 | Spyropoulos et al. (2012) |
| ITO/PEDOT:PSS/P3OT:PCBM /Lif/Al | P3OT:PCBM | 1.1 | 1.7 | Kim and Carroll (2005) |
| ITO/PEDOT:PSS/P3HT:PCBM/LiF/Al | ITO | 1.18 | 1.53 | Shahin et al. (2012) |
| ITO/$TiO_2$/PBDTTT-C-T:$PC_{71}$BM/Ag | PBDTTT-C-T:$PC_{71}$BM | 7.59 | 8.11 | Li et al. (2012) |
| ITO/PEDOT:PSS/P3HT:PCBM/LiF/Al | PEDOT:PSS/ P3HT:PCBM | 3.16 | 3.85 | Xie et al. (2011) |

Please cite this article in press as: Notarianni, M., et al. Plasmonic effect of gold nanoparticles in organic solar cells. Sol. Energy (2013), http://dx.doi.org/10.1016/j.solener.2013.09.026

produced from different thicknesses of gold layers deposited on ITO. Layers of 5 nm, 3 nm and 1 nm of gold were deposited by argon sputtering at $10^{-2}$ mbar on different ITO electrodes followed by annealing at a constant temperature. The annealing process consists in placing the ITO substrates in a tube furnace at 300 °C for 20 min (5 min to ramp up from room temperature to 300 °C) under a 700 cc/min flux of argon. In order to assure the absence of oxygen, the argon was fluxed for 30 min into the furnace with the ITO substrates before starting the annealing procedure and continued until the furnace cooled to 70 °C after the annealing. The SEM images in Fig. 13 shows that at 5 nm and 3 nm gold depositions, the Au NPs are irregularly shaped. As expected, the annealing of the 5 nm gold layer results in larger islands with respect to the 3 nm one. Instead, small particles with round shapes similar to hemispheres are obtained from the 1 nm layer. The distance between individual particles is generally only a few

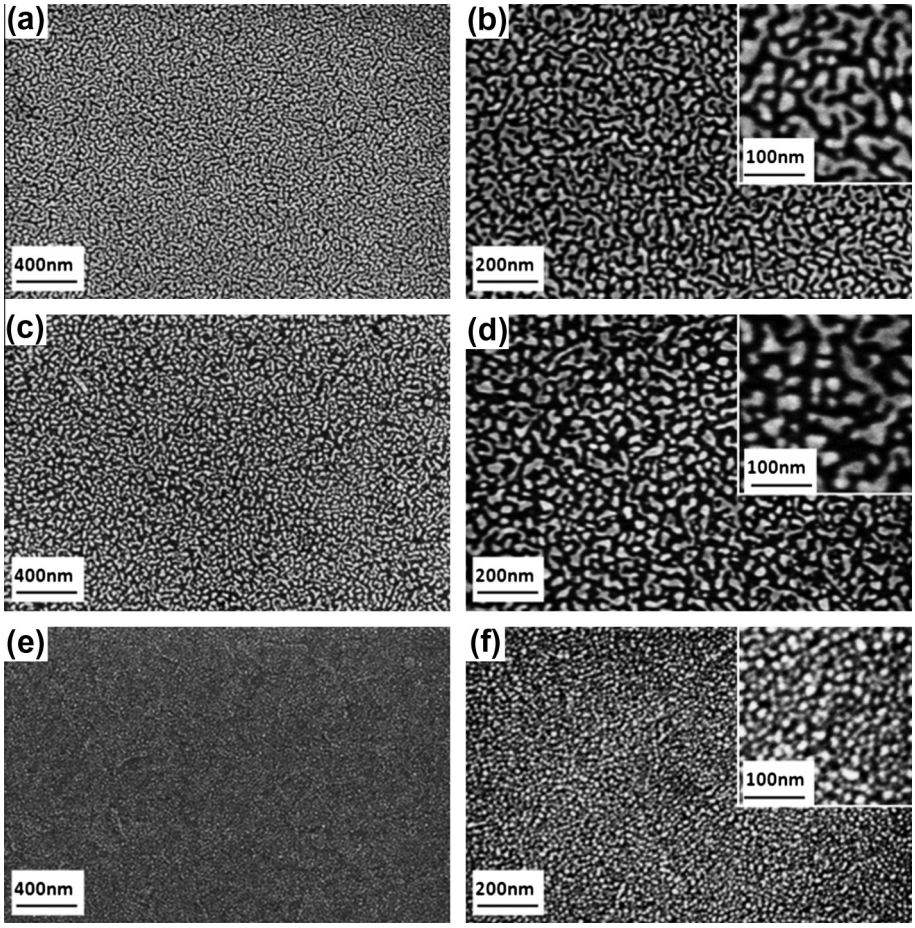


Fig. 13. SEM images of Au NPs grown on ITO by sputtering followed by annealing at 300 °C for 20 min in argon atmosphere. (a and b) 5 nm Au deposition; (c and d) 3 nm Au deposition; (e and f) 1 nm Au deposition.

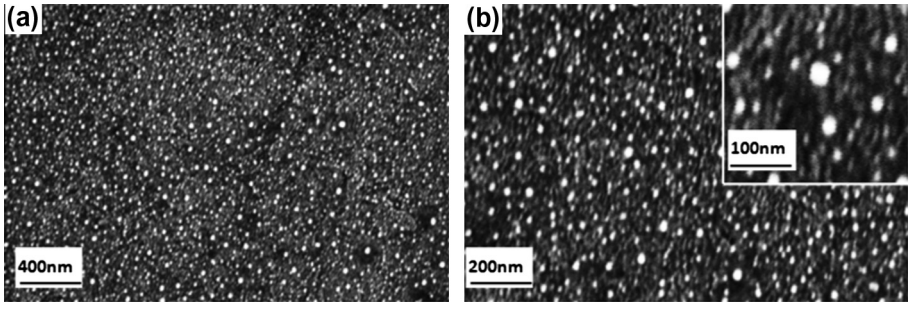


Fig. 14. SEM images of Au NPs grown on ITO. (a and b) Au NPs grown after 1 nm deposition by sputtering of gold through a 25 × 25 mm mask with a regular array of 1 mm holes spaced 1 mm followed by annealing at 300 °C for 20 min in argon atmosphere.

Please cite this article in press as: Notarianni, M., et al. Plasmonic effect of gold nanoparticles in organic solar cells. Sol. Energy (2013), http://dx.doi.org/10.1016/j.solener.2013.09.026

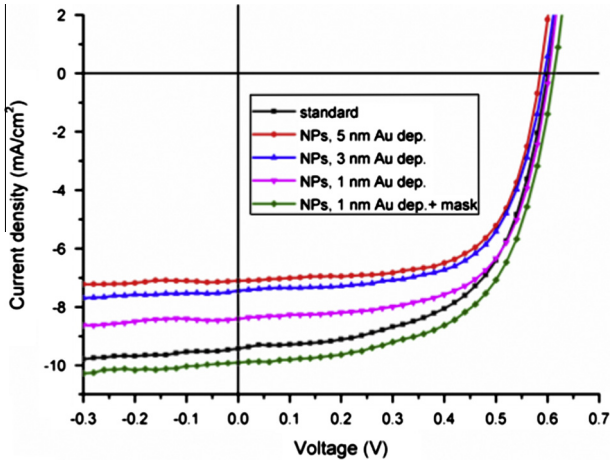


Fig. 15. Current density–voltage characteristics of organic solar cell devices with and without Au NPs grown on ITO by sputtering deposition of gold followed by annealing at 300 °C for 20 min in argon atmosphere. Standard device without Au NPs (black curve); device with Au NPs grown from 5 nm gold deposition (red curve); device with Au NPs grown from 3 nm gold deposition (blue curve); device with Au NPs grown from 1 nm gold deposition (purple curve); device with Au NPs grown from 1 nm gold deposition (green curve). (For interpretation of the references to color in this figure legend, the reader is referred to the web version of this article.)

nanometers but for the 1 nm layer the resulting particles are very compact with a smaller distance between individual particles. A stated earlier, the distance between particles is an important parameter for the performance of an organic solar cell. In fact, the lights is partially reflected by tightly packed NPs decreasing the photoabsorption in the device (Shahin et al., 2012). For this reason, the distance between particles and the embedding medium should be carefully chosen in order to match the wavelength range of the dipole oscillation (Mokkapati et al., 2009). In order to prove this statement, we deposited by sputtering 1 nm of gold on the ITO electrode through a macroscopic aluminum mask with a regular array of 1 mm diameter holes, spaced 1 mm. Then, we annealed the electrodes at 300 °C in a tube furnace with the same procedure described above. SEM images shown in Fig. 14 confirm that, by using the mask, we formed Au NPs with an average size of 40 nm and 20 nm and the distance between the particles increases.

Several devices were made in order to study the effect of the Au NPs size and shape on the device performance. In our experiment, we considered five devices, one standard (100 nm ITO, 20 nm PEDOT:PSS, 100 nm P3HT:PCBM, 80 nm Al), and four plasmonics. The plasmonic devices included Au NPs on top of the ITO electrodes formed by depositing gold layers of 5 nm, 3 nm, 1 nm layers and a 1 nm through a mask of gold respectively, followed by annealing with the same procedure described above.

To fabricate the organic solar cells, ITO coated glass substrates (20 ohms/sq, Xinyan Technology LTD) were cleaned stepwise in deionized water, acetone and isopropyl alcohol under sonication 15 min for each step. The 20 nm layer of PEDOT:PSS (Clevios P VPAI 4083, Heraeus Precious Metals GmbH & Co.) was spin coated onto ITO substrates and annealed at 120 °C for 20 min. Then, a 100 nm of P3HT:$PC_{71}BM$ blend solution dispersed in dichlorobenzene (P3HT, Merck KGaA; $PC_{71}BM$, American Dye Source, Inc.) was spin coated at 1500 rpm for 30 s on the PEDOT:PSS in the nitrogen filled glove box. The 80 nm Al cathode was deposited by thermal evaporation in the nitrogen filled glove box at a chamber pressure of $10^{-6}$ mbar. The devices were then annealed at 170 °C for 2 min on a hot plate before being tested in the solar simulator. Fig. 15 shows the $J$–$V$ characteristic curves recorded under 100 mW/cm$^2$ illumination (AM 1.5G) for the fabricated devices. The active area of the solar cell was 0.2 cm$^2$.

In Table 2, relevant device parameters e.g. open circuit voltage ($V_{oc}$), short circuit current ($J_{sc}$), fill factor (FF), power conversion efficiency (PCE), series resistance ($R_s$) are reported.

The comparison of these devices shows that the PCE and the $J_{sc}$ of the plasmonic devices increases with the decreasing thickness of the gold deposited on the ITO, achieving a PCE of 3.64% when the gold deposited is through the mask. This efficiency is 10% higher than in the case of a standard device without Au NPs.

We infer that the usage of a mask, even macroscopic, reduces the amount of gold that reaches the ITO electrodes by increasing the spacing between the NPs, which results in an increased scattering of the light and in a decreased reflection.

## 7. Conclusions

The restriction on the thickness of the active layer to achieve an efficient charge collection limits the photoabsorption and consequently the power conversion efficiency in organic solar cells. The inclusion of metallic nanoparticles can enhance the photoabsorption by increasing the forward scattering cross section and the near-field enhancement without increasing the thickness of the active

Table 2
Electrical characteristics of the organic solar cell devices incorporating Au NPs on ITO (this work).

| Device | $V_{oc}$ (V) | $J_{sc}$ (mA/cm$^2$) | $R_s$ (Ω cm$^2$) | FF (%) | PCE (%) |
|---|---|---|---|---|---|
| Standard | 0.6 | 9.45 | 11.09 | 59 | 3.35 |
| NPs, 5 nm Au dep. | 0.58 | 7.1 | 12.96 | 66 | 2.74 |
| NPs, 3 nm Au dep. | 0.58 | 7.45 | 15.3 | 66 | 2.84 |
| NPs, 1 nm Au dep. | 0.6 | 8.4 | 11.05 | 64 | 3.24 |
| NPs, 1 nm Au dep. + mask | 0.6 | 9.9 | 12.53 | 61 | 3.64 |

Please cite this article in press as: Notarianni, M., et al. Plasmonic effect of gold nanoparticles in organic solar cells. Sol. Energy (2013), http://dx.doi.org/10.1016/j.solener.2013.09.026

layer. We have examined a number of approaches to produce and include metallic nanoparticles in organic solar cells with a special attention to gold nanoparticles.

By controlling the geometry, the size, the concentration and the placement of the particles, it is possible to enhance the power conversion efficiency in these so called "plasmonic devices".

Including the gold nanoparticles on the ITO by depositing and annealing can be a reproducible and scalable method to fabricate plasmonic devices. It is possible to control the size of the particles by controlling the thickness of the gold deposited and the annealing temperature. The usage of a mask, in order to increase the distance between the particles on the substrate, helps to avoid undesired reflection effects which compromise the efficiency.

In summary we have demonstrated that the right choice of distance and size of the metallic nanoparticles can lead to a dramatic increase of the power conversion efficiency in organic solar cells. Further studies are underway in order to determine the right balance to achieve the best results.

## Acknowledgments

The authors acknowledge the financial support of the Australian Research Council through the Discovery Project DP130102120 and the DP110101454. We also acknowledge the Marie Curie International Research Staff Exchange Scheme Fellowship within the 7th European Community Framework Programme.

We thank the technical support of Dr. P. Hines, Dr. H. Diao and Mr. B. Kwiecien from the Central Analytical Research Facility of the Institute of Future environments at QUT.

This work was performed in part at the Queensland node of the Australian National Fabrication Facility (ANFF) – a company established under the National Collaborative Research Infrastructure Strategy to provide nano and microfabrication facilities for Australia's researchers.

## References

Ameri, T., Dennler, G., Lungenschmied, C., Brabec, C.J., 2009. Organic tandem solar cells: a review. Energy Environ. Sci. 2, 347–363.

Anger, Pascal., Bharadwaj, Palash., Novotny, Lukas., 2006. Enhancement and quenching of single-molecule fluorescence. Phys. Rev. Lett. 96, 113002.

Atwater, Harry A., Polman, Albert, 2010. Plasmonics for improved photovoltaic devices. Nat. Mater. 9, 205–213.

Beck, F.J., Polman, A., Catchpole, K.R., 2009. Tunable light trapping for solar cells using localized surface plasmons. J. Appl. Phys. 105, 114310–114317.

Bernardi, M., Giulianini, M., Grossman, J.C., 2010. Self-assembly and its impact on interfacial charge transfer in carbon nanotube/P3HT solar cells. ACS Nano 4, 6599–6606.

Bindl, D.J., Wu, M.Y., Prehn, F.C., Arnold, M.S., 2011. Efficiently harvesting excitons from electronic type-controlled semiconducting carbon nanotube films. Nano Lett. 11, 455–460.

Bohren, Craig, F., 1983. How can a particle absorb more than the light incident on it? Am. J. Phys. 51, 323–327.

Bohren, C.F., Huffman, D.R., 2008. Absorption and Scattering of Light by Small Particles. Wiley.

Brabec, C.J., Durrant, J.R., 2008. Solution-processed organic solar cells. MRS Bull. 33, 670–675.

Bundgaard, E., Krebs, F.C., 2007. Low band gap polymers for organic photovoltaics. Sol. Energy Mater. Sol. Cells 91, 954–985.

Capasso, A., Salamandra, L., Di Carlo, A., Bell, J.M., Motta, N., 2012. Low-temperature synthesis of carbon nanotubes on indium tin oxide electrodes for organic solar cells. Beilstein J. Nanotechnol. 3, 524–532.

Catchpole, K.R., Polman, A., 2008a. Design principles for particle plasmon enhanced solar cells. Appl. Phys. Lett. 93, 191113–191123.

Catchpole, K.R., Polman, A., 2008b. Plasmonic solar cells. Opt. Express 16, 21793–21800.

Catchpole, K.R., Mokkapati, S., Beck, F., Wang, E.C., McKinley, A., Basch, A., Lee, J., 2011. Plasmonics and nanophotonics for photovoltaics. MRS Bull. 36, 461–467.

Chen, Fang-Chung, Wu, Jyh-Lih, Lee, Chia-Ling, Hong, Yi, Kuo, Chun-Hong, Huang, Michael H., 2009. Plasmonic-enhanced polymer photovoltaic devices incorporating solution-processable metal nanoparticles. Appl. Phys. Lett. 95, 013305–013313.

Cheng, Yunan, Stakenborg, Tim, Van Dorpe, Pol, Lagae, Liesbet, Wang, Mang, Chen, Hongzheng, Borghs, Gustaaf, 2011. Fluorescence near gold nanoparticles for DNA sensing. Anal. Chem. 83, 1307–1314.

Chou, Alison, Vernon, Kristy C., Piro, Lennart, Radi, Babak, Jaatinen, Esa A., Davis, Timothy J., 2012. Predicting the localized surface plasmon resonances of spherical nanoparticles on a substrate: electrostatic eigenmode method. J. Phys. Chem. C 116, 26517–26522.

Dabera, G.Dinesha M.R., Jayawardena, K.D.G.Imalka, Prabhath, M.R.Ranga, Yahya, Iskandar, Tan, Y.Yuan, Nismy, N.Aamina, Shiozawa, Hidetsugu, Sauer, Markus, Ruiz-Soria, G., Ayala, Paola, Stolojan, Vlad, Adikaari, A.A.Damitha T., Jarowski, Peter D., Pichler, Thomas, Silva, S.Ravi P., 2012. Hybrid carbon nanotube networks as efficient hole extraction layers for organic photovoltaics. ACS Nano 7, 556–565.

Dang, Minh Trung, Hirsch, Lionel, Wantz, Guillaume, 2011. P3HT:PCBM, best seller in polymer photovoltaic research. Adv. Mater. 23, 3597–3602.

Dennler, Gilles, Scharber, Markus C., Brabec, Christoph J., 2009. Polymer–fullerene bulk-heterojunction solar cells. Adv. Mater. 21, 1323–1338.

Derkacs, D., Lim, S.H., Matheu, P., Mar, W., Yu, E.T., 2006. Improved performance of amorphous silicon solar cells via scattering from surface plasmon polaritons in nearby metallic nanoparticles. Appl. Phys. Lett. 89, 093103–093113.

Derkacs, D., Chen, W.V., Matheu, P.M., Lim, S.H., Yu, P.K.L., Yu, E.T., 2008. Nanoparticle-induced light scattering for improved performance of quantum-well solar cells. Appl. Phys. Lett. 93, 091107–091113.

Dou, L., You, J., Yang, J., Chen, C.C., He, Y., Murase, S., Moriarty, T., Emery, K., Li, G., Yang, Y., 2012. Tandem polymer solar cells featuring a spectrally matched low-bandgap polymer. Nat. Photon. 6, 180–185.

Duche, David, Torchio, Philippe, Escoubas, Ludovic, Monestier, Florent, Simon, Jean-Jacques, Flory, François, Mathian, Gérard, 2009. Improving light absorption in organic solar cells by plasmonic contribution. Sol. Energy Mater. Sol. Cells 93, 1377–1382.

Erb, T., Zhokhavets, U., Gobsch, G., Raleva, S., Stühn, B., Schilinsky, P., Waldauf, C., Brabec, C.J., 2005. Correlation between structural and optical properties of composite polymer/fullerene films for organic solar cells. Adv. Funct. Mater. 15, 1193–1196.

Etchegoin, P., Cohen, L.F., Hartigan, H., Brown, R.J.C., Milton, M.J.T., Gallop, J.C., 2004. Localized plasmon resonances in inhomogeneous metallic nanoclusters. Chem. Phys. Lett. 383, 577–583.

Frens, G., 1973. Controlled nucleation for the regulation of the particle size in monodisperse gold suspensions. Nature 241, 20–22.

Please cite this article in press as: Notarianni, M., et al. Plasmonic effect of gold nanoparticles in organic solar cells. Sol. Energy (2013), http://dx.doi.org/10.1016/j.solener.2013.09.026

Frondelius, P., Häkkinen, H., Honkala, K., 2010. Formation of gold(I) edge oxide at flat gold nanoclusters on an ultrathin MgO film under ambient conditions. Angew. Chem. – Int. Ed. 49, 7913–7916.

Giulianini, M., Waclawik, E.R., Bell, J.M., Scarselli, M., Castrucci, P., De Crescenzi, M., Motta, N., 2009. Poly(3-hexyl-thiophene) coil-wrapped single wall carbon nanotube investigated by scanning tunneling spectroscopy. Appl. Phys. Lett. 95.

Giulianini, M., Waclawik, E.R., Bell, J.M., Crescenzi, M.D., Castrucci, P., Scarselli, M., Diociauti, M., Casciardi, S., Motta, N., 2011a. Evidence of multiwall carbon nanotube deformation caused by poly(3-hexylthiophene) adhesion. J. Phys. Chem. C 115, 6324–6330.

Giulianini, M., Waclawik, E.R., Bell, J.M., Scarselli, M., Castrucci, P., De Crescenzi, M., 2011b. Microscopic and spectroscopic investigation of poly(3-hexylthiophene) interaction with carbon nanotubes. Polymers 3, 1433–1446.

Grancini, G., Maiuri, M., Fazzi, D., Petrozza, A., Egelhaaf, H.J., Brida, D., Cerullo, G., Lanzani, G., 2013. Hot exciton dissociation in polymer solar cells. Nat. Mater. 12, 29–33.

Hadipour, A., de Boer, B., Blom, P.W.M., 2008. Device operation of organic tandem solar cells. Org. Electron.: Phys., Mater., Appl. 9, 617–624.

Haiss, Wolfgang, Thanh, Nguyen T.K., Aveyard, Jenny, Fernig, David G., 2007. Determination of size and concentration of gold nanoparticles from UV−Vis spectra. Anal. Chem. 79, 4215–4221.

Halls, J.J.M., Pichler, K., Friend, R.H., Moratti, S.C., Holmes, A.B., 1996. Exciton diffusion and dissociation in a poly(p-phenylenevinylene)/C[sub 60] heterojunction photovoltaic cell. Appl. Phys. Lett. 68, 3120–3122.

Hamasha, M.M., Dhakal, T., Alzoubi, K., Albahri, S., Qasaimeh, A., Lu, S., Westgate, C.R., 2012. Stability of ITO thin film on flexible substrate under thermal aging and thermal cycling conditions. IEEE/OSA J. Display Technol. 8, 383–388.

Hau, S.K., Yip, H.L., Jen, A.K.Y, 2010. A review on the development of the inverted polymer solar cell architecture. Polym. Rev. (Philadelphia, PA, US) 50, 474–510.

Heliatek Firm, 2013. Heliatek consolidates technology leadership by establishing a new world record for organic solar technology with a cell efficiency of 12% (press release). Heliatek, Dresden, Germany.

Huffman, D.R., Bohren, C.F. 1983. Absorption and Scattering of Light by Small Particles. New York.

Jain, Prashant K., Lee, Kyeong Seok, El-Sayed, Ivan H., El-Sayed, Mostafa A., 2006. Calculated absorption and scattering properties of gold nanoparticles of different size, shape, and composition: applications in biological imaging and biomedicine. J. Phys. Chem. B 110, 7238–7248.

Jørgensen, Mikkel, Norrman, Kion, Krebs, Frederik C., 2008. Stability/degradation of polymer solar cells. Sol. Energy Mater. Sol. Cells 92, 686–714.

Kalowekamo, Joseph., Baker, Erin., 2009. Estimating the manufacturing cost of purely organic solar cells. Sol. Energy 83, 1224–1231.

Kambhampati, Patanjali, 2011. Hot exciton relaxation dynamics in semiconductor quantum dots: radiationless transitions on the nanoscale. J. Phys. Chem. C 115, 22089–22109.

Kang, Myung-Gyu, Xu, Ting, Park, Hui Joon, Luo, Xiangang, Jay Guo, L., 2010. Efficiency enhancement of organic solar cells using transparent plasmonic Ag nanowire electrodes. Adv. Mater. 22, 4378–4383.

Kao, C.S., Chen, F.C., Liao, C.W., Huang, M.H., Hsu, C.S., 2012. Plasmonic-enhanced performance for polymer solar cells prepared with inverted structures. Appl. Phys. Lett. 101, 193902–193904.

Kelly, K.Lance, Coronado, Eduardo, Zhao, Lin Lin, Schatz, George C., 2002. The optical properties of metal nanoparticles: the influence of size, shape, and dielectric environment. J. Phys. Chem. B 107, 668–677.

Kim, Kyungkon, Carroll, David L., 2005. Roles of Au and Ag nanoparticles in efficiency enhancement of poly(3-octylthiophene)/C[sub 60] bulk heterojunction photovoltaic devices. Appl. Phys. Lett. 87, 203113–203123.

Kim, Y.N., Shin, H.G., Song, J.K., Cho, D.H., Lee, H.S., Jung, Y.G., 2005. Thermal degradation behavior of indium tin oxide thin films deposited by radio frequency magnetron sputtering. J. Mater. Res. 20, 1574–1579.

Kim, Seok-Soon, Na, Seok-In, Jo, Jang, Kim, Dong-Yu, Nah, Yoon-Chae, 2008. Plasmon enhanced performance of organic solar cells using electrodeposited Ag nanoparticles. Appl. Phys. Lett. 93, 073307–073313.

Kippelen, B., Brédas, J.L., 2009. Organic photovoltaics. Energy Environ. Sci. 2, 251–261.

Kirchartz, T., Agostinelli, T., Campoy-Quiles, M., Gong, W., Nelson, J., 2012. Understanding the thickness-dependent performance of organic bulk heterojunction solar cells: The influence of mobility, lifetime, and space charge. J. Phys. Chem. Lett. 3, 3470–3475.

Krebs, F.C., 2009a. All solution roll-to-roll processed polymer solar cells free from indium–tin-oxide and vacuum coating steps. Org. Electron.: Phys., Mater., Appl. 10, 761–768.

Krebs, Frederik C., 2009b. Fabrication and processing of polymer solar cells: a review of printing and coating techniques. Sol. Energy Mater. Sol. Cells 93, 394–412.

Krebs, Frederik C. 2010. Polymeric Solar Cells: Materials, Design, Manufacture.

Kreibig, U., Vollmer, M., 1995. Optical Properties of Metal Clusters. Springer.

Lee, Ji Hwang, Park, Jong Hwan, Kim, Jong Soo, Lee, Dong Yun, Cho, Kilwon, 2009. High efficiency polymer solar cells with wet deposited plasmonic gold nanodots. Org. Electron. 10, 416–420.

Lee, Kwan.H., Schwenn, Paul.E., Arthur, R.G., Smith, Hamish Cavaye, Shaw, Paul E., James, Michael, Krueger, Karsten B., Gentle, Ian R., Meredith, Paul, Burn, Paul L., 2011. Morphology of all-solution-processed "bilayer" organic solar cells. Adv. Mater. 23, 766–770.

Li, G., Shrotriya, V., Huang, J., Yao, Y., Moriarty, T., Emery, K., Yang, Y., 2005. High-efficiency solution processable polymer photovoltaic cells by self-organization of polymer blends. Nat. Mater. 4, 864–868.

Li, X., Choy, W.C.H., Huo, L., Xie, F., Sha, W.E.I., Ding, B., Guo, X., Li, Y., Hou, J., You, J., Yang, Y., 2012. Dual plasmonic nanostructures for high performance inverted organic solar cells. Adv. Mater. 24, 3046–3052.

Liang, Yongye, Feng, Danqin, Wu, Yue, Tsai, Szu-Ting, Li, Gang, Ray, Claire, Yu, Luping, 2009. Highly efficient solar cell polymers developed via fine-tuning of structural and electronic properties. J. Am. Chem. Soc. 131, 7792–7799.

Liang, Yongye, Zheng, Xu., Xia, Jiangbin, Tsai, Szu-Ting, Wu, Yue, Li, Gang, Ray, Claire, Yu, Luping, 2010. For the bright future—bulk heterojunction polymer solar cells with power conversion efficiency of 7.4%. Adv. Mater. 22, E135–E138.

Lin, Su-Jien, Lee, Kuang-Che, Wu, Jyun-Lin, Wu, Jun-Yi, 2012. Plasmon-enhanced photocurrent in dye-sensitized solar cells. Sol. Energy 86, 2600–2605.

Lindquist, Nathan C., Luhman, Wade A., Oh, Sang-Hyun, Holmes, Russell J., 2008. Plasmonic nanocavity arrays for enhanced efficiency in organic photovoltaic cells. Appl. Phys. Lett. 93, 123308–123313.

Louis, Catherine, Pluchery, Olivier. 2012. Gold Nanoparticles for Physics, Chemistry and Biology.

Lu, Luyao, Luo, Zhiqiang, Xu, Tao, Yu, Luping, 2012. Cooperative plasmonic effect of Ag and Au nanoparticles on enhancing performance of polymer solar cells. Nano Lett. 13, 59–64.

Lu, Luyao, Xu, Tao, Wei Chen, Lee, Ju Min, Luo, Zhiqiang, Jung, In Hwan, Park, Hyung Il, Kim, Sang Ouk, Yu, Luping, 2013. The role of N-doped multiwall carbon nanotubes in achieving highly efficient polymer bulk heterojunction solar cells. Nano Lett. 13, 2365–2369.

Maier, Stefan A., 2007. Plasmonics: Fundamentals and Applications. Springer, New York.

Mariani, G., Laghumavarapu, R.B., Tremolet De Villers, B., Shapiro, J., Senanayake, P., Lin, A., Schwartz, B.J., Huffaker, D.L., 2010. Hybrid conjugated polymer solar cells using patterned GaAs nanopillars. Appl. Phys. Lett. 97, 013107–013113.

Mertz, Jerome, 2000. Radiative absorption, fluorescence, and scattering of a classical dipole near a lossless interface: a unified description. J. Opt. Soc. Am. B 17, 1906–19013.

Please cite this article in press as: Notarianni, M., et al. Plasmonic effect of gold nanoparticles in organic solar cells. Sol. Energy (2013), http://dx.doi.org/10.1016/j.solener.2013.09.026

Mihailetchi, V.D., Koster, L.J.A., Blom, P.W.M., Melzer, C., De Boer, B., Van Duren, J.K.J., Janssen, R.A.J., 2005. Compositional dependence of the performance of poly(p-phenylene vinylene):methanofullerene bulk-heterojunction solar cells. Adv. Funct. Mater. 15, 795–801.

Min Nam, Y., Huh, J., Ho Jo, W., 2010. Optimization of thickness and morphology of active layer for high performance of bulk-heterojunction organic solar cells. Sol. Energy Mater. Sol. Cells 94, 1118–1124.

Mirri, Francesca, Anson, W.K., Ma, Tienyi T., Hsu, Natnael Behabtu, Eichmann, Shannon L., Young, Colin C., Tsentalovich, Dmitri E., Pasquali, Matteo, 2012. High-performance carbon nanotube transparent conductive films by scalable dip coating. ACS Nano 6, 9737–9744.

Mokkapati, S., Catchpole, K.R., 2012. Nanophotonic light trapping in solar cells. J. Appl. Phys. 112, 101101–101119.

Mokkapati, S., Beck, F.J., Polman, A., Catchpole, K.R., 2009. Designing periodic arrays of metal nanoparticles for light-trapping applications in solar cells. Appl. Phys. Lett. 95, 053115–053123.

Morfa, Anthony J., Rowlen, Kathy L., Reilly, Thomas H., Romero, Manuel J., van de Lagemaat., Jao, 2008. Plasmon-enhanced solar energy conversion in organic bulk heterojunction photovoltaics. Appl. Phys. Lett. 92, 013504–013513.

Muduli, Subas, Game, Onkar, Dhas, Vivek, Vijayamohanan, K., Bogle, K.A., Valanoor, N., Ogale, Satishchandra B., 2012. TiO2–Au plasmonic nanocomposite for enhanced dye-sensitized solar cell (DSSC) performance. Sol. Energy 86, 1428–1434.

Namkoong, G., Kong, J., Samson, M., Hwang, I.W., Lee, K., 2013. Active layer thickness effect on the recombination process of PCDTBT:PC71BM organic solar cells. Org. Electron.: Phys., Mater., Appl. 14, 74–79.

Nelson, J., 2011. Polymer: fullerene bulk heterojunction solar cells. Mater. Today 14, 462–470.

Niggemann, M., Glatthaar, M., Gombert, A., Hinsch, A., Wittwer, V., 2004. Diffraction gratings and buried nano-electrodes—architectures for organic solar cells. Thin Solid Films 451–452, 619–623.

Nunzi, J.M., 2002. Organic photovoltaic materials and devices. C. R. Phys. 3, 523–542.

Ohkita, Hideo, Cook, Steffan, Astuti, Yeni, Duffy, Warren, Tierney, Steve, Zhang, Weimin, Heeney, Martin, McCulloch, Iain, Nelson, Jenny, Bradley, Donal D.C., Durrant, James R., 2008. Charge carrier formation in polythiophene/fullerene blend films studied by transient absorption spectroscopy. J. Am. Chem. Soc. 130, 3030–3042.

Peet, J., Kim, J.Y., Coates, N.E., Ma, W.L., Moses, D., Heeger, A.J., Bazan, G.C., 2007. Efficiency enhancement in low-bandgap polymer solar cells by processing with alkane dithiols. Nat. Mater. 6, 497–500.

Pelton, M., Aizpurua, J., Bryant, G., 2008. Metal-nanoparticle plasmonics. Laser Photon. Rev. 2, 136–159.

Pillai, S., Catchpole, K.R., Trupke, T., Green, M.A., 2007. Surface plasmon enhanced silicon solar cells. J. Appl. Phys. 101, 093105–093118.

Pivrikas, A., Neugebauer, H., Sariciftci, N.S., 2011. Influence of processing additives to nano-morphology and efficiency of bulk-heterojunction solar cells: a comparative review. Sol. Energy 85, 1226–1237.

Powell, Colin, Bender, Timothy, Lawryshyn, Yuri, 2009. A model to determine financial indicators for organic solar cells. Sol. Energy 83, 1977–19784.

Rand, Barry P., Peumans, Peter, Forrest, Stephen R., 2004. Long-range absorption enhancement in organic tandem thin-film solar cells containing silver nanoclusters. J. Appl. Phys. 96, 7519–7526.

Ren, S., Bernardi, M., Lunt, R.R., Bulovic, V., Grossman, J.C., Gradečak, S., 2011. Toward efficient carbon nanotube/P3HT solar cells: Active layer morphology, electrical, and optical properties. Nano Lett. 11, 5316–5321.

Sanchez, A., Abbet, S., Heiz, U., Schneider, W.D., Häkkinen, H., Barnett, R.N., Landman, U., 1999. When gold is not noble: nanoscale gold catalysts. J. Phys. Chem. A 103, 9573–9578.

Sariciftci, N.S., Smilowitz, L., Heeger, A.J., Wudl, F., 1992. Photoinduced electron transfer from a conducting polymer to buckminsterfullerene. Science 258, 1474–1476.

Schilinsky, Pavel., Waldauf, Christoph., Brabec, Christoph.J., 2002. Recombination and loss analysis in polythiophene based bulk heterojunction photodetectors. Appl. Phys. Lett. 81, 3885–3887.

Sears, K., Fanchini, G., Watkins, S.E., Huynh, C.P., Hawkins, S.C., 2013. Aligned carbon nanotube webs as a replacement for indium tin oxide in organic solar cells. Thin Solid Films.

Seemann, Andrea, Sauermann, Tobias, Lungenschmied, Christoph, Armbruster, Oskar, Bauer, Siegfried, Egelhaaf, H.J., Hauch, Jens, 2011. Reversible and irreversible degradation of organic solar cell performance by oxygen. Sol. Energy 85, 1238–1249.

Sgobba, V., Guldi, D.M., 2008. Carbon nanotubes as integrative materials for organic photovoltaic devices. J. Mater. Chem. 18, 153–157.

Shahin, S., Gangopadhyay, P., Norwood, R.A., 2012. Ultrathin organic bulk heterojunction solar cells: plasmon enhanced performance using Au nanoparticles. Appl. Phys. Lett., 101.

Shen, Honghui, Bienstman, Peter, Maes, Bjorn, 2009. Plasmonic absorption enhancement in organic solar cells with thin active layers. J. Appl. Phys. 106, 073109–073115.

Smestad, Greg P., Krebs, Frederik C., Lampert, Carl M., Granqvist, Claes G., Chopra, K.L., Mathew, Xavier, Takakura, Hideyuki, 2008. Reporting solar cell efficiencies in Solar Energy Materials and Solar Cells. Sol. Energy Mater. Sol. Cells 92, 371–373.

Spyropoulos, George D., Stylianakis, Minas M., Stratakis, Emmanuel, Kymakis, Emmanuel, 2012. Organic bulk heterojunction photovoltaic devices with surfactant-free Au nanoparticles embedded in the active layer. Appl. Phys. Lett. 100, 213904–213915.

Street, R.A., Schoendorf, M., Roy, A., Lee, J.H., 2010. Interface state recombination in organic solar cells. Phys. Rev. B – Condens. Matter Mater. Phys. 81.

Su, Y.W., Lan, S.C., Wei, K.H., 2012. Organic photovoltaics. Mater. Today 15, 554–562.

Sun, Yanming, Gong, Xiong, Hsu, Ben B.Y., Yip, Hin-Lap, Jen, Alex K.Y., Heeger, Alan J., 2010. Solution-processed cross-linkable hole selective layer for polymer solar cells in the inverted structure. Appl. Phys. Lett. 97, 193310–193323.

Sutter, E.A., Tong, X., Jungjohann, K., Sutter, P.W., 2013. Oxidation of nanoscale Au–In alloy particles as a possible route toward stable Au-based catalysts. Proc. Natl. Acad. Sci. USA 110, 10519–10524.

Tao, C., Aljada, M., Shaw, P.E., Lee, K.H., Cavaye, H., Balfour, M.N., Borthwick, R.J., James, M., Burn, P.L., Gentle, I.R., Meredith, P., 2013. Controlling hierarchy in solution-processed polymer solar cells based on crosslinked P3HT. Adv. Energy Mater. 3, 105–112.

Theander, M., Yartsev, A., Zigmantas, D., Sundström, V., Mammo, W., Andersson, M.R., Inganäs, O., 2000. Photoluminescence quenching at a polythiophene/$C_{60}$ heterojunction. Phys. Rev. B 61, 12957–12963.

Topp, K., Borchert, H., Johnen, F., Tunc, A.V., Knipper, M., Von Hauff, E., Parisi, J., Al-Shamery, K., 2010. Impact of the incorporation of Au nanoparticles into polymer/fullerene solar cells. J. Phys. Chem. A 114, 3981–3989.

Turkevich, J., Stevenson, P.C., Hillier, J., 1951. A study of the nucleation and growth processes in the synthesis of colloidal gold. Discuss. Faraday Soc. 11, 55–75.

Umnov, A.G., Korovyanko, O.J., 2005. Photovoltaic effect in poly-dioctyl-phenylene-ethynylene-C[sub 60] cells upon donor and acceptor excitation. Appl. Phys. Lett. 87, 113506–113513.

van Dijk, M.A., Tchebotareva, A.L., Orrit, M., Lippitz, M., Berciaud, S., Lasne, D., Cognet, L., Lounis, B., 2006. Absorption and scattering microscopy of single metal nanoparticles. Phys. Chem. Chem. Phys. 8, 3486–3495.

Viktor Andersson, B., Wuerfel, Uli, Inganäs, Olle, 2011. Full day modelling of V-shaped organic solar cell. Sol. Energy 85, 1257–1263.

Wang, C.C.D., Choy, W.C.H., Duan, C., Fung, D.D.S., Sha, W.E.I., Xie, F.X., Huang, F., Cao, Y., 2012. Optical and electrical effects of gold nanoparticles in the active layer of polymer solar cells. J. Mater. Chem. 22, 1206–1211.

Please cite this article in press as: Notarianni, M., et al. Plasmonic effect of gold nanoparticles in organic solar cells. Sol. Energy (2013), http://dx.doi.org/10.1016/j.solener.2013.09.026

Wang, J., Lee, Y.J., Chadha, A.S., Yi, J., Jespersen, M.L., Kelley, J.J., Nguyen, H.M., Nimmo, M., Malko, A.V., Vaia, R.A., Zhou, W., Hsu, J.W.P., 2013. Effect of plasmonic Au nanoparticles on inverted organic solar cell performance. J. Phys. Chem. C 117, 85–91.

Watkins, P.K., Walker, A.B., Verschoor, G.L.B., 2005. Dynamical monte carlo modelling of organic solar cells: the dependence of internal quantum efficiency on morphology. Nano Lett. 5, 1814–1818.

Wong, Kim Hai, Ananthanarayanan, Krishnamoorthy, Heinemann, Marc Daniel, Luther, Joachim, Balaya, Palani, 2012. Enhanced photocurrent and stability of organic solar cells using solution-based NiO interfacial layer. Sol. Energy 86, 3190–3195.

Woo, S., Jeong, J.H., Lyu, H.K., Han, Y.S., Kim, Y., 2012. In situ-prepared composite materials of PEDOT:PSS buffer layer-metal nanoparticles and their application to organic solar cells. Nanoscale Res. Lett. 7, 641–647.

Wu, Jyh-Lih, Chen, Fang-Chung, Hsiao, Yu-Sheng, Chien, Fan-Ching, Chen, Peilin, Kuo, Chun.-Hong., Huang, Michael H., Hsu, Chain-Shu, 2011. Surface plasmonic effects of metallic nanoparticles on the performance of polymer bulk heterojunction solar cells. ACS Nano 5, 959–967.

Xie, Feng-Xian, Choy, Wallace C.H., Wang, Charlie.C.D., Sha, Wei E.I., Fung, Dixon D.S., 2011. Improving the efficiency of polymer solar cells by incorporating gold nanoparticles into all polymer layers. Appl. Phys. Lett. 99, 153304–153313.

Xu, Mei-Feng, Zhu, Xiao-Zhao, Shi, Xiao-Bo, Liang, Jian, Jin, Yue, Wang, Zhao-Kui, Liao, Liang-Sheng, 2013. Plasmon resonance enhanced optical absorption in inverted polymer/fullerene solar cells with metal nanoparticle-doped solution-processable TiO2 layer. ACS Appl. Mater. Interfaces 5, 2935–2942.

Yang, Guowei, 2012. Laser Ablation in Liquids – Principles and Applications in the Preparation of Nanomaterials. Pan Stanford.

Yang, Jun, You, Jingbi, Chen, Chun-Chao, Hsu, Wan-Ching, Tan, Hai.-ren., Zhang, XingWang, Hong, Ziruo., Yang, Yang, 2011. Plasmonic polymer tandem solar cell. ACS Nano 5, 6210–6217.

You, J., Dou, L., Yoshimura, K., Kato, T., Ohya, K., Moriarty, T., Emery, K., Chen, C.C., Gao, J., Li, G., Yang, Y., 2013. A polymer tandem solar cell with 10.6% power conversion efficiency. Nat. Commun. 4.

Zeng, Beibei, Gan, Qiaoqiang, Kafafi, Zakya H., Bartoli, Filbert J., 2013. Polymeric photovoltaics with various metallic plasmonic nanostructures. J. Appl. Phys. 113, 063109–063110.

Zhu, Zhengguo, Waller, David, Gaudiana, Russell, Morana, Mauro, Mühlbacher, David, Scharber, Markus, Brabec, Christoph, 2007. Panchromatic conjugated polymers containing alternating donor/acceptor units for photovoltaic applications. Macromolecules 40, 1981–1986.

Zhu, Hongwei, Wei, Jinquan, Wang, Kunlin, Wu, Dehai, 2009. Applications of carbon materials in photovoltaic solar cells. Sol. Energy Mater. Sol. Cells 93, 1461–1470.

Please cite this article in press as: Notarianni, M., et al. Plasmonic effect of gold nanoparticles in organic solar cells. Sol. Energy (2013), http://dx.doi.org/10.1016/j.solener.2013.09.026